Improved Adaptation Speed of the Robust Fixed Point Transformation-based Controller Using Virtual Response Forecast

Bence Varga

Doctoral School of Applied Informatics and Applied Matehmatics,
Banki Donat Faculty of Mechanical and Safety Engineering,
Obuda University, H-1034 Budapest, Bécsi út 96/B, Hungary
E-mail: varga.bence@bgk.uni-obuda.hu
ORCID: 0000-0002-4739-8680

Richárd Horváth

Banki Donat Faculty of Mechanical and Safety Engineering,
Obuda University, H-1034 Budapest, Bécsi út 96/B, Hungary
E-mail: horvath.richard@bgk.uni-obuda.hu
ORCID: 0000-0002-4924-3244

József K. Tar

Doctoral School of Applied Informatics and Applied Matehmatics,
John von Neumann Faculty of Informatics,
Obuda University, H-1034 Budapest, Bécsi út 96/B, Hungary
E-mail: tar.jozsef@nik.uni-obuda.hu
ORCID: 0000-0002-5476-401X

Abstract: Robust Fixed Point Transformation-based adaptive control design was introduced in 2009, in order to overcome some of the difficulties of certain Lypunov function-based adaptive control design techniques. This control method was developed for trajectory tracking applications for nonlinear second order systems. The RFPT controller, instead of refining some kind of available dynamic model, that is neiter precise nor complete, targets the deterministic behavior of the trajectory tracking error, by finding the correct control signal in an iterative manner. In each control cycle a single step of iteration is made. In this paper a variation of the RFPT control method is introduced, where concurrent adaptive control and model identification is applied, based on Recursive Least Square Algorithm and a Hammerstein model. In the proposed control scheme the estimated control response is used to apply multiple iterative steps, that way increasing the adaptation speed of the controller. The proposed solution was tested on experimental basis in a DC motor control application. The increased adaptation speed of the proposed method resulted in more precise trajectory tracking.

Keywords: Robust Fixed Point Transformation; Hammerstein Model; Recursive Least Square Algorithm; Adaptive Control.

1 Introduction

The development of adaptive control techniques commenced in the 1950s, with initial applications in servo systems [1] and flight control [2]. In these early stages the MIT-rule was widely used in Model Reference Adaptive Control (MRAC) design, however it became apparent that this method is prone to unexpected instability [3, 4]. Although the theoretical foundation for stability analysis was already established by Lyapunov [5, 6] at the end of the 19th century, the first practical implementations in the adaptive control framework was only introduced in the 60s e.g., one of the pioneering work was published by Parks et al. [7]. In his work the gradient search method used for control parameter tuning in the MIT-rule was replaced with a Lyapunov function based tuning procedure in an MRAC design. Since then, Lyapunov function based adaptive control design techniques became one of the most popular tools in MRAC, e.g. [8, 9], and in countless other methods that have been developed over the last few decades for adaptive control of nonlinear systems [10]. Such as, some classic approaches as Adaptive Inverse Dynamics [11, 12] or Slotine Li Adaptive Control [13], that was developed in field of robotics or the backstepping method [14] that got great deal of attention in the recent years [15, 16].

In 2009 a Robust Fixed Point Transformation-based (RFPT) adaptive control design was introduced [17]. This iterative control method was developed for trajectory tracking applications, where a sufficiently smooth nominal trajectory ($q^N(t)$) must be precisely followed by a nonlinear second order system such as a CNC machine or a robot. However, over the years various application areas were investigated for applying Fixed Point Iteration-based (FPI) adaptive control techniques, such as anesthesiology [18, 19], treating diabetes [20, 21], classical mechanical systems [22], controlling DC motors [23], neuron models [24, 25]. The main motivation behind the development of RFPT method is to overcome some of the design difficulties of the Lyapunov function-based techniques, that is summarized in [17] as:

- During the design process of such controller the Lyapunov function ($V(x(t),t)$) is constructed as function of various states ($x(t)$). For stability analysis the non-increasing nature of $\dot{V} < 0$ (for asymptotic stability) must be proven. However, from $\dot{V} < 0$ we cannot conclude for the elements of x that the property $\frac{\mathrm{d}|x_i|}{\mathrm{d}t} < 0$ would be valid. So the system states may change in various manner, that is not desirable e.g., in life science applications;
- The control method concentrates on the asymptotic stability of the controller and the behavior of the system in the initial transient phase is overshadowed. That might be unacceptable in some applications, again e.g., in life sciences. Although some methods exist, such as e.g., adaptive funnel control to ensure transient behavior [26].

To avoid these problems, the RFPT controller places in the center of attention definite behavior of the trajectory tracking error, that is the difference between the nominal ($q^N(t)$) and realized trajectory of the system ($q^R(t)$), $e(t) = q^N(t) - q^R(t)$. Essentially this control method is an adaptive variation of Computed Torque Control (CTC) [27, 28] that is widely used in robotics. The stucture of the controller is shown in Fig. 1.

In CTC method the desired trajectory of the second derivative of the generalized coordinates ($\ddot{q}^{Des}(t)$) is calculated purely on kinematic basis e.g., using a simple PID (Proportional-Integral-Derivative) feedback rule. In order to linearize and decouple the nonlinear dynamics of the controlled system the inverse dynamic model is used to calculate the control force to be exerted on the system, $Q(t) = F^{-1}(q(t), \dot{q}(t), \ddot{q}^{Des}(t))$. However, it became apparent in the 90s that it is practically impossible to develop a precise dynamic model for control purposes [29]. So the available imprecise inverse dynamic model ($\tilde{F}^{-1}(\cdot)$) results in

$$\ddot{q}^R(t) = F(q(t), \dot{q}(t), \tilde{Q}(t)) \neq \ddot{q}^{Des}(t) \tag{1}$$

where $F(\cdot)$ is the function of the actual system dynamics and $\tilde{Q}(t)$ denotes the generalized force that includes the disturbance and the control force, too, that was calculated based on the imprecise dynamic model.

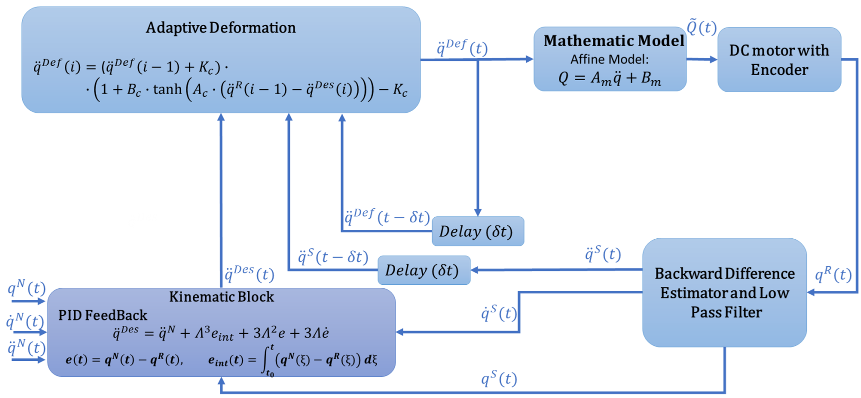

Figure 1
RFPT control schematics for a DC motor with encoder based position measurement and backward difference estimator with low pass filter

The RFPT control method was inspired by Banach's Fixed Point Theorem [30], that states that a contractive function $f : \mathscr{B} \mapsto \mathscr{B}$ which generates a sequence as $\{x_0, x_1 = f(x_0) \ldots x_n = f(x_{n-1})\}$ that converges to the unique fixed point $x_* = f(x_*)$, where $\mathscr{B}$ is linear, complete metric space, a Banach Space. The basic idea of RFPT control is that instead of refining the available imprecise model, it applies an iterative solution to find the control force $Q(t)$ that would result in $\ddot{q}^R(t) \approx \ddot{q}^{Des}(t)$ system response. Essentially the control task is transformed to a Fixed Point Problem and by the use of Contractive Mapping a sequence is generated that converges to the solution of the control task. In practice it means that instead of $\ddot{q}^{Des}(t)$ a deformed value ($\ddot{q}^{Def}(t)$) is generated using an appropriate deformation function, as $\ddot{q}^{Def}(t) = G(\ddot{q}^{Des}(t), \ddot{q}^{Def}(t-\delta t), \ddot{q}^R(t-\delta t))$ and the $q^{Def}(t)$ is used to calculate the control force resulting in

$$\ddot{q}^R(t) = F(q(t), \dot{q}(t), \tilde{F}^{-1}(q^R(t), \dot{q}^R(t), \ddot{q}^{Def}(t))) \approx \ddot{q}^{Des}(t) \quad . \tag{2}$$

So $\ddot{q}^{Def}(t)$ is found in an iterative manner, where in each control cycle a single step of iteration is made, with the initial condition $\ddot{q}^{Def}(0) = \ddot{q}^{Des}(0)$. Compared to CTC in RFPT control, in case of a 2nd order system, not only the first order derivative but also the second order derivative is fed back with some delay δt, that usually corresponds to the sampling time of the digital controller. For the implementation detail of the adaptive deformation function ($G(\cdot)$) various methods can be found besides that was proposed in [17]. For example the solution was extended for MIMO systems [31, 32]. In [33] a so called "Abstract Rotations" method is introduced based on a simple geometric interpretation to replace $G(\cdot)$, in order to make the controller tuning process easier. In order to address noise sensitivity of the solution a continuous variant of $G(\cdot)$ is suggested in [34] based on the idea of Luenberger observer [35]. The RFPT control was also implemented in an MRAC framework in [36]. Further advantage of FPI control is that it can be combined with many different control approaches. For example in [37, 38] the simple PID rule in the kinematic block was replaced by fractional order inspired feedback solution, that was characterized by a finite memory length to improve control performance. In similar manner, in place of the kinematic block a Control Lyapunov Function was introduced in [39]. It was also shown that it can enhance the control performance of various Lyapunov function based control design as Adaptive Inverse Dynamics [40], Slotine-Li Adaptive Control [41] or the backstepping method [42].

In conclusion the following properties of the RFPT method inspired the current article:

- the RFPT controller does not make any effort to identify the controlled system. Instead of that it applies an iterative approach to find the control force that results in sufficient trajectory tacking performance. Although, in recent years some methods were suggested for FPI control and concurrent model identification e.g., in [43, 44] Particle Swarm Optimization algorithm and in [45] a simple Least Squares Fit method was used to identify the model parameters. In both cases it was assumed that the mathematical form of the model was precisely known, and only the model parameters were adjusted;

- the adaptive deformation used in RFPT method can compensate for various modeling deficiencies. It was shown in [46] that even the simplest affine model in form of $\tilde{Q}(t) = A\ddot{q}^{Def}(t) + B$, where A and B are the model parameters, can result in sufficient control performance in certain applications. In [46] this property of the RFPT method was exploited to avoid state estimation for an under-actuated system;

- in FPI control in each control cycle a single step of iteration is made, so the convergence rate of the iterative process, and also the tracking precision is limited by the sampling time (δt) of the controller. Although, in [47, 48, 49] Steffensen's method was applied in an FPI controller to accelerate the convergence of the iteration.

The novelties introduced in this paper are twofold. At first model identification process of a nonlinear Hammerstein model using Recursive Least Squares (RLS) algorithm is applied in an RFPT adaptive control scenario. Furthermore, on the basis of the already identified model form during one digital control step more than one fictive iterative steps are applied for the calculation of the necessary adaptive deformation. The proposed method is tested on experimental basis, in a simple DC motor control application.

This paper is organized in the following manner. In Section 2 some implementation details of the RFPT controller is introduced, with special emphasis on the formulation of the kinematic prescription for $\ddot{q}^{Des}(t)$ and the adaptive deformation function. In Section 3 the Hammerstein Model and the RLS algorithm is introduced and applied in the RFPT control framework. Section 4 presents the experimental results and finally in Section 5 the conclusions are summarized.

2 Robust Fixed Point Transformation

The error relaxation rule of RFPT control can be formulated in various manners. One potential solution is to implement the following prescription

$$\left(\Lambda+\frac{\mathrm{d}}{\mathrm{dt}}\right)^3 e_{int}(t)=0 \ , \tag{3}$$

for the integrated trajectory tracking error ($e_{int}(t)=\int_{t_0}^{t}\left[q^N(\xi)-q^R(\xi)\right]\mathrm{d}\xi$). Considering that $\ddot{e}(t)=\ddot{q}^N(t)-\ddot{q}(t)$, the desired value of the 2nd order derivative of the generalized coordinates is given as

$$\ddot{q}^{Des}(t)=\ddot{q}^N(t)+\Lambda^3 e_{int}(t)+3\Lambda^2 e(t)+3\Lambda\dot{e}(t) \ , \tag{4}$$

where $\Lambda>0$ is a single design parameter and $K_p=3\Lambda^2$, $K_i=\Lambda^3$, $K_d=3\Lambda$ are the PID gains of the controller. The solution of (3) as an LTI (Linear Time Invariant) system can be written as linear combination of 3 exponential terms

$$e_{int}(t)=\sum_{\ell=0}^{2} c_\ell (t-t_0)^\ell \exp(-\Lambda(t-t_0)) \ , \tag{5}$$

in which the $\{c_0,c_1,c_2\}$ parameters are determined by the initial conditions. Evidently, from (5) it is easy to see that in some time, depending on the control parameter Λ, $e_{int}(t)\to 0$ as $t\to\infty$. In similar manner the decreasing nature of $e(t)$ and $\dot{e}(t)$ can be seen, considering that (5) can be rewritten as,

$$\left(\Lambda+\frac{\mathrm{d}}{\mathrm{dt}}\right)^3 e_{int}(t)=\left(\Lambda+\frac{\mathrm{d}}{\mathrm{dt}}\right)\left[\left(\Lambda+\frac{\mathrm{d}}{\mathrm{dt}}\right)^2 e_{int}(t)\right]=0 \ , \text{ that leads to} \tag{6}$$

$$\left(\Lambda+\frac{\mathrm{d}}{\mathrm{dt}}\right)^2 e_{int}(t)=\left(\Lambda+\frac{\mathrm{d}}{\mathrm{dt}}\right)\left[\left(\Lambda+\frac{\mathrm{d}}{\mathrm{dt}}\right) e_{int}(t)\right]=0 \ , \text{ and finally} \tag{7}$$

$$\left(\Lambda+\frac{\mathrm{d}}{\mathrm{dt}}\right) e_{int}(t)=0 \text{ from which again } e_{int}(t)=0 \ . \tag{8}$$

Equation (7) gives us $\left(\Lambda+\frac{\mathrm{d}}{\mathrm{dt}}\right)e(t)=-\Lambda e_{int}(t)$, in which the inhomogeneous part will vanish in some time, considering that $e_{int}(t)\to 0$ as $t\to\infty$. So it can be concluded that $e(t)\to 0$ as $t\to\infty$. In similar manner from (6) we can write that

$\left(\Lambda+\frac{\mathrm{d}}{\mathrm{dt}}\right)\dot{e}(t)=-\Lambda^2 e_{int}(t)-2\Lambda e(t)$ and again we can conclude that $\dot{e}(t)$ will converge to zero as $t\to\infty$ as well, because of the fact that $e_{int}(t)$, $e(t)\to 0$ as $t\to\infty$, . Finally, it is evident that by precisely implementing $\ddot{q}^{Des}(t)$ not only $e_{int}(t)$, but also $e(t)$ and $\dot{e}(t)$ will converge to 0 in some time.

However, without the precise inverse dynamic model of the controlled system, it is practically impossible to precisely implement $\ddot{q}^{Des}(t)$ as it was shown in Section 1. In case of RFPT control an adaptive deformation is applied on the desired value. In [17] the suggested deformation function, assuming that a digital controller is used for implementation, where the control force is applied on the system in deterministic manner over a time grid $t\in\{0,\delta t,2\delta t,...,k\delta t\}$

$$\ddot{q}^{Def}(t)=\left(K_c+\ddot{q}^{Def}(t-\delta t)\right)\left[1+B_c\tanh\left(A_c\left(\ddot{q}^R(t-\delta t)-\ddot{q}^{Des}(t)\right)\right)\right]-K_c \quad . \tag{9}$$

In (9) the A_c, B_c and K_c parameters must be tuned by the user based on the following considerations. If $\ddot{q}^{Def}(t)<\ddot{q}^{Def}(t+\delta t)$ results in $\ddot{q}^R(t)<\ddot{q}^R(t+\delta t)$ where,

$$\ddot{q}^R(t)=F(q(t),\dot{q}(t),\tilde{F}^{-1}(q^R(t),\dot{q}^R(t),\ddot{q}^{Def}(t))) \text{ and} \tag{10}$$

$$\ddot{q}^R(t+\delta t)=F(q(t+\delta t),\dot{q}(t+\delta t),\tilde{F}^{-1}(q^R(t+\delta t),\dot{q}^R(t+\delta t),\ddot{q}^{Def}(t+\delta t))) \tag{11}$$

then $F(\cdot)$ is an increasing function so $B_c=-1$. Furthermore, due to the saturation of the function $tanh(\cdot)$, in the initial phase of the control when $\ddot{q}^R(t-\delta t)\gg\ddot{q}^{Des}(t)$ the $G(\cdot)$ deformation function in (9) will approximate $-K_c$. On the other hand, if $\ddot{q}^R(t-\delta t)\ll\ddot{q}^{Des}(t)$, $G(\cdot)$ will approximate the $2\ddot{q}^{Def}(t-\delta t)+K_c$ affine function. Essentially, in case of a sufficiently large K_c value, the system will be driven towards $\ddot{q}^{Des}(t)$ with a constant control force, due to the increasing nature of $F(\cdot)$. Similar considerations can be made for decreasing $F(\cdot)$ functions as well, with $B_c=1$. In close vicinity of the fixed point, when $\ddot{q}^{Def}(t-\delta t)=\ddot{q}_*(t)\pm\varepsilon$, $\varepsilon\in\mathbb{R}_+$, the contractivity of (9) must be ensured by proper tuning of parameter A_c.

A function $f:\mathscr{B}\mapsto\mathscr{B}$ is contractive if $|f(a)-f(b)|\le\beta|a-b|$ with $0\le\beta<1$. Such function will generate a convergent Cauchy Sequence in a Banach space (Banach's Fixed Point Theorem, see Section 1). To guarantee the contractivity of $f(\cdot)$, its derivative must satisfy that $|f'(\cdot)|\le\beta<1$, since

$$|f(a)-f(b)|=\left|\int_a^b f'(x)\mathrm{dx}\right|\le\int_a^b|f'(x)|\mathrm{dx}\le\beta|\mathrm{a}-\mathrm{b}| \quad . \tag{12}$$

The derivative of (9) is given as

$$G'(\cdot)=\left(1+B_c\tanh(A_c(F(\cdot)-\ddot{q}^{Des}(t)))\right)+\left(\frac{(\ddot{q}^{Def}(t-\delta t)+K_c)B_cA_cF'(\cdot)}{\cosh^2(A_c(F(\cdot)-\ddot{q}^{Des}(t))}\right) \tag{13}$$

where $\ddot{q}^R(t-\delta t)=F(q(t-\delta t),\dot{q}(t-\delta t),\tilde{F}^{-1}(q^R(t-\delta t),\dot{q}^R(t-\delta t),\ddot{q}^{Def}(t-\delta t)))=F(\cdot)$. For an increasing function $F(\cdot)$ $F'(\cdot)>0$, and since K_c is a large value, while $B_c=-1$, A_c must be a sufficiently small e.g., it can be redefined a A_c/K_c, to ensure that $|G'(\cdot)|<1$. Equation (13) reveals also limitation of RFPT control as well, since if the system dynamics is fast (high $F'(\cdot)$) compared to the iteration process we cannot ensure that $|G'(\cdot)|<1$ so the iteration will become divergent. Essentially, this means that with the feedback of $\ddot{q}^R(t-\delta t)$ we do not gain any useful insight on the system dynamics as it changes too fast. In practice, this could make it harder to control systems that have dead-zone nonlinearities or stick-slip behaviour. This is because the iteration might temporarily become different during certain parts of the control process. The optimal parameter setting of the RFPT method was investigated in [50].

3 Model identification in RFPT control

Most mechanical and electro-mechanical systems, such as robots or even a simple DC motor exhibit some kind of nonlinear behavior, stemming from friction phenomena [51], actuator dead-zone [52] or backlash of the drive system [53, 54] etc., that must be compensated by the controller. These nonlinear phenomena makes the identification and control of such systems more difficult. To capture the essence of these nonlinearities various, sometimes quite complex models have been developed and applied in control applications over the years such as, LuGre friction model [55]. Other methods rather utilize some kind of general model form e.g., Hammerstein model [56] tuned purely from input-output measurements, in order to capture the nonlinearities of the controlled system. The latter solution seems to be advantageous in an RFPT control design, since it does not require heavy work from the control designer as the development of complex models with various nonlinear components and the RFPT method can be considered as quasi data driven control approach. It was also shown in [57] that the Hammerstein model can capture various nonlinearities that are the characteristics of electro-mechanical systems.

3.1 Introducing the Hammerstein Model

The Hammerstein model has a simple structure, which consists of a static input nonlinearity and a dynamic linear subsystem as shown on Fig. 2. The nonlinear part is often represented with a polynomial function [57, 58, 59]

$$u(t) = \gamma_1 Q(t) + \gamma_2 Q^2(t) + \ldots + \gamma_n Q^n(t) \quad , \tag{14}$$

where γ_i, $i \in \{1,2,\ldots,n\}$ are the coefficients of the nonlinear block, $u(t)$ is an internal signal of the model that serves as an input to the linear subsystem. The linear part can be designed in various manners as well, a plausible and widely used solution (e.g., [57, 60]) is an ARX (Autoregressive Exogenous) model

$$\begin{aligned}\ddot{q}^R(t) + \alpha_1\ddot{q}^R(t-\delta t) + \alpha_2\ddot{q}^R(t-2\delta t) + \ldots + \alpha_{n_a}\ddot{q}^R(t-n_a\delta t) = \\ = \beta_0 u(t) + \beta_1 u(t-\delta t) + \beta_2 u(t-2\delta t) + \ldots + \beta_{n_b} u(t-n_b\delta t) \quad .\end{aligned} \tag{15}$$

By combining (14) and (15)

$$\ddot{q}^R(t) = \sum_{j=0}^{n_b}\sum_{k=1}^{n} \beta_j\gamma_k Q^k(t-j\delta t) - \sum_{\ell=1}^{n_a} \alpha_\ell \ddot{q}^R(t-\ell\delta t) \quad , \tag{16}$$

$$\ddot{q}^R(t) = \sum_{j=0}^{n_b} \beta_j Q(t-j\delta t) + \sum_{j=0}^{n_b}\sum_{k=2}^{n} \beta_j\gamma_k Q^k(t-j\delta t) - \sum_{\ell=1}^{n_a} \alpha_\ell \ddot{q}^R(t-\ell\delta t) \quad . \tag{17}$$

Finally, (17) results in a linear regression form as

$$\ddot{q}^R(t) = \psi^T(t)\Theta(t) \tag{18}$$

where $\Theta(t) = \left[-\alpha_1 \ \ldots - \alpha_{n_a} \ \ \beta_0 \ \ldots \beta_{n_a} \ \ \kappa_{02} \ \ldots \kappa_{n_b 2} \ \ \kappa_{0n} \ \ldots \kappa_{n_b n}\right]$ is the parameter array with $\kappa_{jk} = \beta_j \gamma_k$, $j \in \{0, 1, \ldots, n_b\}$, $k \in \{2, 3, \ldots, n\}$ and

$$\psi^T(t) = [\ddot{q}^R(t-\delta t) \ \ldots \ddot{q}^R(t - n_a \delta t) \ \ Q(t) \ \ldots Q(t - n_b \delta t)$$
$$Q^2(t) \ \ldots Q^2(t - n_b \delta t) \ \ldots Q^n(t) \ \ldots Q^n(t - n_b \delta t)]$$

is the observation array, that contains only the measurable signals. The advantage of the regression form in (18) is that the $\Theta(t)$ parameter matrix can be simply estimated using a Recursive Least Squares (RLS) Algorithm [61].

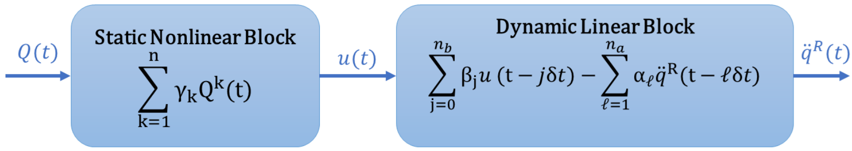

Figure 2
Hammerstein model structure

3.2 Recursive Least Square Algorithm

Lets introduce $\tilde{\Theta}(t)$, that is the estimate of the model parameters in (18). Then, utilizing various input-output measurement data ($\psi^T(t)$) the system response can be estimated as

$$\ddot{q}^E(t) = \psi^T(t)\tilde{\Theta}(t) \ . \tag{19}$$

The update law for the parameter estimate can be formulated based on the Least Square method by introducing the estimation error $\varepsilon(t) = \ddot{q}^R(t) - \ddot{q}^E(t)$ and

$$S = \frac{1}{2}\sum_{k=0}^{m}\left(\ddot{q}^R(t-k\delta t) - \ddot{q}^E(t-k\delta t)\right)^2 =$$
$$= \frac{1}{2}\sum_{k=0}^{m}\left(\ddot{q}^R(t-k\delta t) - \psi^T(t-k\delta t)\tilde{\Theta}(t-k\delta t)\right)^2 \ , \tag{20}$$

$m = \frac{t}{\delta t}$ and minimizing S as $\frac{\partial S}{\partial \theta_i} = 0$, resulting in

$$\tilde{\Theta}(t) = (\Psi^T(t)\Psi(t))^{-1}\Psi^T(t)Y(t) \ , \tag{21}$$

where $\Psi(t) = \left[\psi^T(t - m\delta t) \ \ldots \ \psi^T(t-\delta t) \ \ \psi^T(t)\right]$ and $Y(t) = \left[\ddot{q}^R(t - m\delta t) \ \ldots \ \ddot{q}^R(t-\delta t) \ \ \ddot{q}^R(t)\right]$. However, the calculation of $(\Psi^T(t)\Psi(t))^{-1}$ is computationally demanding and it seems reasonable, especially in case of digital controllers, that instead of recalculating $\tilde{\Theta}(t)$ in each control cycle, use an update law that utilizes $\tilde{\Theta}(t-\delta t)$ and the estimation error of $q^E(t) =$

$\psi^T(t)\tilde{\Theta}(t-\delta t)$. Such method is called Recursive Least Square Algorithm and it is widely used in adaptive control and system identification [61, 62]. The RLS method works under the assumption that $P(t) = \Psi^T(t)\Psi(t)$ is non singular and it has inverse for all t, so (21) can be rewritten as

$$\tilde{\Theta}(t) = P(t)\sum_{k=0}^{m}\left(\psi(t-m\delta t)\ddot{q}^R(t-m\delta t)\right) =$$
$$= P(t)(\sum_{k=1}^{m}\left(\psi(t-m\delta t)\ddot{q}^R(t-m\delta t)\right) + \psi(t)\ddot{q}^R(t)) \quad . \quad (22)$$

Utilizing that

$$P^{-1}(t) = \sum_{k=0}^{m}\psi(t-k\delta t)\psi^T(t-k\delta t) = \overbrace{\sum_{k=1}^{m}\psi(t-k\delta t)\psi^T(t-k\delta t)}^{P(t-\delta t)} + \psi(t)\psi^T(t) \quad , \quad (23)$$

and (21)

$$\sum_{k=1}^{m}\psi(t-m\delta t)\ddot{q}^R(t-m\delta t) = P(t-\delta t)\tilde{\Theta}(t-\delta t) =$$
$$= P^{-1}(t)\tilde{\theta}(t-\delta t) - \psi(t)\psi^T(t)\tilde{\Theta}(t-\delta t) \quad . \quad (24)$$

Now substituting (24) into (22) we get that

$$\tilde{\Theta}(t) = \tilde{\Theta}(t-\delta t) + P(t)\psi(t)\left(\ddot{q}^R(t) - \psi^T(t)\tilde{\Theta}(t-\delta t)\right) =$$
$$= \tilde{\Theta}(t-\delta t) + P(t)\psi(t)\left(\ddot{q}^R(t) - \ddot{q}^E(t)\right) \quad , \quad (25)$$

which is the model parameter update law for the RLS algorithm. Furthermore, by applying the Sherman-Morrison-Woodbury formula, that is $(A+BCD)^{-1} = A^{-1} - A^{-1}B\left(C^{-1}+DA^{-1}B\right)^{-1}DA^{-1}$ with $A = P^{-1}(t-\delta t)$, $B = D^T = \psi(t)$, $C = 1$ on the inverse of (23)

$$P(t) = P(t-\delta t)\left(I_p - \frac{\psi(t)\psi^T(t)P(t-\delta t)}{1-\psi^T(t)P(t-\delta t)\psi(t)}\right) \quad , \quad (26)$$

where I_p is an identity matrix of same dimensions as $P(t)$. From (25) and (26) it is evident that both $\tilde{\Theta}(t)$ and $P(t)$ are updated in a recursive manner, which is computationally more efficient than the matrix inversion in (21) that is good for online identification.

3.3 Proposed Multiple Step RFPT Control

In this paper a novel RFPT control design is introduced that is supported by an online identification of a nonlinear Hammerstein model. The structure of the proposed modification is given in Fig. 3. The essence of the method is that the model parameters of (18) are recursively updated in each control cycle using (25) and (26), in order to "learn" the system dynamics $\psi^T(t)\tilde{\Theta}(t-\delta t) \approx F(q(t),\dot{q}(t),Q(t))$. Then in each control cycle, the identified model is employed to implement a series of iterative steps. The subsequent section of the paper introduces new notation. The number in the subscript of any variable indicates the number of the iterative step to which the quantity corresponds to. For-example, $\ddot{q}_i^{Def}(t)$ is the deformed value of the second derivative of the generalized coordinates after the i$^{\text{th}}$ iterative step at time t. In the proposed solution the adaptive deformation is modified as

$$\ddot{q}_i^{Def}(t) = \begin{cases} G(\ddot{q}^{Des}(t), \ddot{q}^{Def}(t-\delta t), \ddot{q}^R(t-\delta t)) & \text{if } i=1 \\ G(\ddot{q}^{Des}(t), \ddot{q}_{i-1}^{Def}(t), \ddot{q}_{i-1}^E(t)) & \text{if } i>1 \end{cases} \quad \text{where} \ , \tag{27}$$

$$\ddot{q}_i^E(t) = \psi^T(t)\tilde{\Theta}(t-\delta t) \ ; \tag{28}$$

and $i \in \{1,2,....,s\}$, $s \in \mathbb{N}$ is set by the user. Essentially instead of introducing $\ddot{q}_1^{Def}(t)$, that is the deformed value after a single step of iteration, into the approximate dynamic model, the iteration is virtually continued in the future using the same approximate model and the the identified Hammerstein model (28) to forecast the system response. After making $s \in \mathbb{N}$ virtual steps in the future, in the control program the latest deformed value is placed into the variable $\ddot{q}_s^{Def}(t)$, and the control is continued by the use of this improved deformed value. In this manner, instead using only one adaptive parameter A_c that must be as large as possible to achieve fast convergence in vicinity of the fixed point, the adaptivity can be made finer by using a smaller A_c parameter with a few forecasting steps s. The concurrent application of the model parameter identification and RFPT control ensures precise tracking from the beginning of the control, while trajectory tracking precision will be further improved over time.

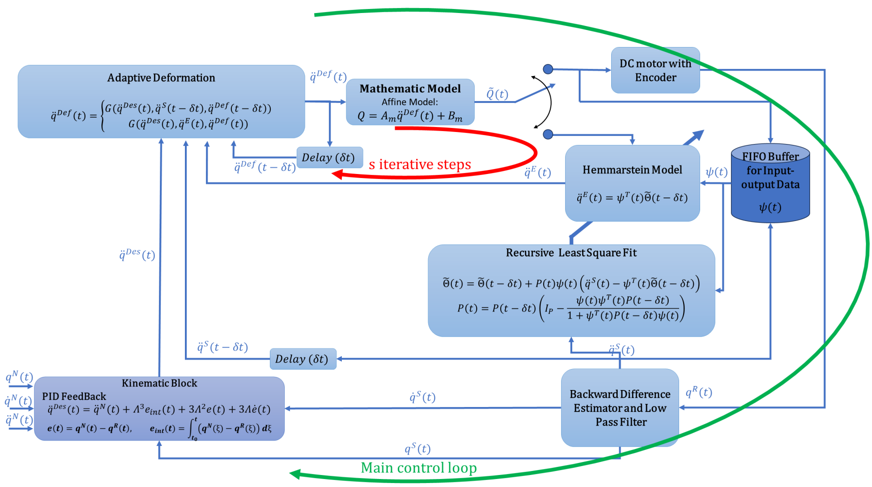

Figure 3
Improved RFPT control with model identification and multiple adaptive steps

The expectation that in this manner some improvement can be achieved is based on the experience that there exist several data driven techniques that are able to build up some useful model of the controlled system by fresh observations. In these techniques certain generally valid structures can be "filled in" with the observed data so that these general structures are not related to any specialties of the observed system. For instance, Petriu in [64] distinguished between three main types as generally model-free controllers (e.g., [65]), virtual reference feedback tuning-based controllers (e.g., [66]), and model-free adaptive controllers (e.g., [[67], [68]]). In [69] the abstract rotations-based formalism was suggested to create a formal structure to be used by the data driven techniques. Fényes et al., e.g., used pace regression for using noise filtered signals for the estimation of the quality of road surfaces and tire pressure in [70, 71]. His idea is akin to our proposal to use the fitted model form in (28). In this paper a simple experimental validation is made for the proposed control solution with a DC motor and the results are presented in the next section.

4 Experimental Results

The proposed solution was subjected to experimental testing in a DC motor control application. The FIT0185-type 12 VDC motor is equipped with an incremental encoder and a planetary gearbox. The encoder resolution is 16 pulses per motor revolution; however, due to the 1:131 reduction ratio of the planetary gearbox, 2096 pulses can be counted during one output shaft revolution. This number was further increased by a factor of four using quadrature decoding of both encoder channels. The motor shaft was connected to a spring and the disturbance force exerted by it can be expressed as,

$$Q_L(t) = \theta_w \ddot{q}(t) + D_s l_e l_t \sin q(t) \left(1 - \frac{l_{r0}}{\sqrt{l_e^2 + l_t^2 - 2 l_e l_t \cos q(t)}}\right) , \tag{29}$$

where θ_w is the inertia of the coupling, D_s is the spring constant, l_e denotes the length of the lever on which the loading torque of the spring is applied, l_t is the distance between the fixed mounting point of the spring and the motor shaft and finally l_{r0} is the length of the spring corresponding to $q = 0$ angular motor position. (shown in Fig. 4).

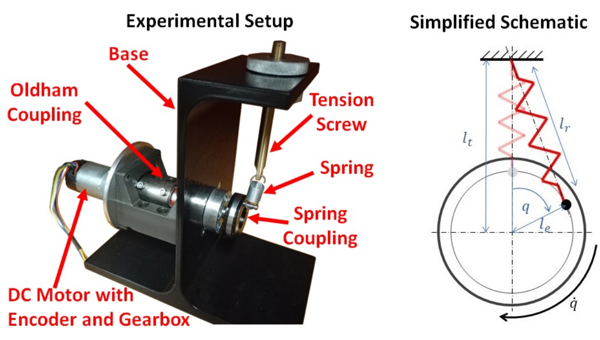

Figure 4
Mechanical design of the experimental setup (left) and simplified dynamic model (right)

A simple block diagram of the experimental setup is given in Fig. 5. The control algorithm was implemented on a Teensy 4.0 development board equipped with ARM Cortex-M7 processor. The adaptive deformation was applied on the PWM (Pulse Width Modulation) output of the controller. The output shaft position of the motor ($q^R(t)$) was measured using the inbuilt encoder and higher derivatives ($\dot{q}^R(t)$, $\ddot{q}^R(t)$) were estimated using second order backward difference formulae,

$$\dot{q}^R(t) = \frac{3q^R(t) - 4q^R(t-\delta t) + q^R(t-2\delta t)}{2\delta t} \quad , \tag{30}$$

$$\ddot{q}^R(t) = \frac{2q^R(t) - 5q^R(t-\delta t) + 4q^R(t-2\delta t) - q^R(t-3\delta t)}{\delta t^2} \quad . \tag{31}$$

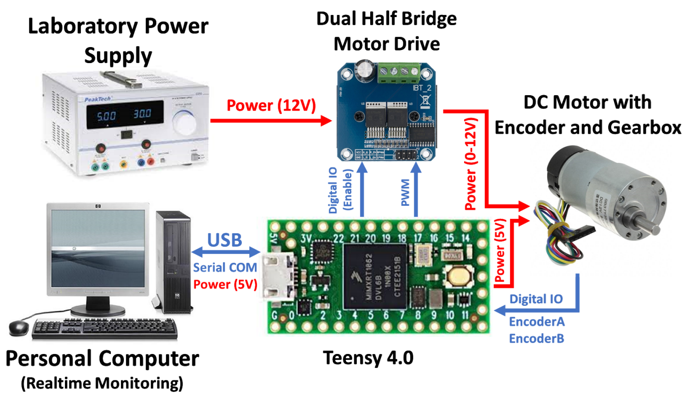

Figure 5
Simple Block Diagram of the Experimental Setup

The noisy signals were filtered using a simple digital implementation of an IIR (Infinite Impulse Response) low pass filter design [63]

$$\dot{q}^S(t) = \mathfrak{b}\dot{q}^S(t-\delta t) + \mathfrak{a}(\dot{q}^R(t) + \dot{q}^R(t-\delta t)) \quad , \tag{32}$$

$$\ddot{q}^S(t) = \mathfrak{b}\ddot{q}^S(t-\delta t) + \mathfrak{a}(\ddot{q}^R(t) + \ddot{q}^R(t-\delta t)) \quad . \tag{33}$$

The control objective was to precisely track a sinusoidal nominal trajectory given as

$$q^N(t) = A_t \cos(\omega_t t) \tag{34}$$

where $A_t = 4\pi$ and $\omega_t = 2\pi 0.1$. The low pass filter parameters were $\mathfrak{b} = 0.90999367$ and $\mathfrak{a} = 0.04500317$ that corresponds to a $f_c = 15Hz$ cut-off frequency. The Hammerstein model parameters were $n = 2$ for the static nonlinear block and $n_a = n_b = 3$ for the dynamic linear subsystem. For the recursive identification process in (25) and (26), $\tilde{\Theta}(0) = [0\ \ 0\ \ \ldots\ \ 0]$ and $P(0) = P_0 I_p$ with $P_0 = 100$ initial values were used. The design parameter for (4) kinematic prescription was chosen $\Lambda = 15\ \mathrm{s}^{-1}$, while the adaptive parameters in (9) were $B_c = -1$, $K_c = 1000000\ \mathrm{s}^{-2}$ and finally

$A_c = \frac{0.5}{K_c}$. In case of the proposed multiple step variant of the RFPT method in each control cycle $s = 3$ adaptive steps were made. The approximate inverse dynamic model ($\tilde{F}^{-1}(\cdot)$)

$$Q_{PWM}(t) = A_m \ddot{q}_s^{Def}(t) + B_m \tag{35}$$

where the model parameters are simply set as $A_m = 1$ and $B_m = 0$, essentially directly converting $\ddot{q}_s^{Def}(t)$ to PWM value in order to control the H-bridge used for driving the motor. The adaptive deformation was applied to the system after the 1500th control step, and in the first 12500 control cycle only a single step of iteration was made.

Table 1
Control Performance Indices for all Experimental Measurements

No	Spring Load	Step Count	e_{max}	μ_e	σ_e
1	No Spring Attached	1	0.00423	0.00046	0.00042
2			0.00487	0.00050	0.00049
3			0.00497	0.00050	0.00049
4			0.00528	0.00055	0.00052
5			0.00584	0.00058	0.00061
6		3	0.00296	0.00052	0.00037
7			0.00230	0.00049	0.00035
8			0.00345	0.00051	0.00036
9			0.00164	0.00043	0.00031
10			0.00258	0.00053	0.00038
11	Spring Attached	1	0.00708	0.00083	0.00091
12			0.00793	0.00076	0.00094
13			0.00831	0.00076	0.00096
14			0.00814	0.00078	0.00097
15			0.00819	0.00076	0.00096
16		3	0.00303	0.00055	0.00040
17			0.00268	0.00054	0.00039
18			0.00289	0.00057	0.00042
19			0.00284	0.00053	0.00038
20			0.00201	0.00047	0.00033

In the testing procedure, 20 consecutive measurements were made in different configuration that are summarized in Table 1. For comparison purposes the following control performance indices were introduced:

- Maximum absolute tracking error: $e_{max} = \max\limits_{i=1,2,..,N}(|e(i)|)$;
- Average absolute tracking error: $\mu_e = \frac{1}{N}\sum_{i=1}^{N}|e(i)|$;
- Standard deviation of the trajectory tracking error: $\sigma_e = \sqrt{\frac{1}{N}\sum_{i=1}^{N}(|e(i)| - \mu_e)^2}$.

The performance indexes were calculated only for the $25-40s$ interval, that way eliminating the effects of the transient phase. From Fig. 6 we can see that after a relatively short transient phase a precise trajectory tracking was achieved. In this scenario the spring was not applied on the shaft of the motor. On the left-hand side of the figure, $q^N(t)$ and $q^R(t)$ values are displayed and the quantization error of the position measurement can be observed. As it is shown in the right-hand side of Fig. 6, the control performance is mainly improved in the low velocity regime where actuator dead-zone and stick-slip effect appear. These observations are also supported by the findings presented in Table 1 as the average (μ_e) and the deviation (σ_e) of the trajectory tracking error are within the same range for the unloaded motor. However, the maximum of the absolute trajectory tracking error exhibits a decline with the increase in the number of iterative steps.

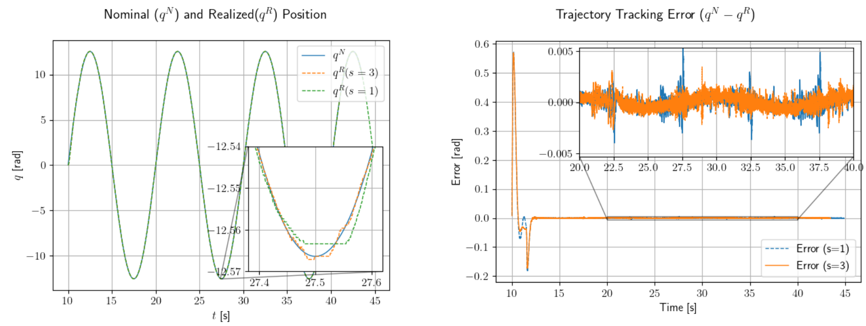

Figure 6
Angular Position of the output shaft of the DC motor (left) and trajectory tracking error (right) - s denotes the number of iterative steps in each control cycle

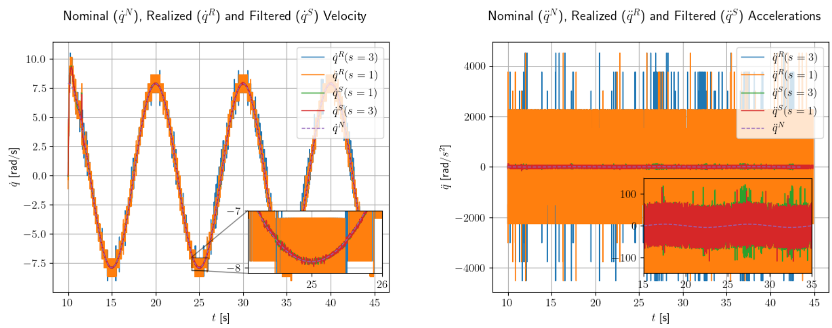

Figure 7
Angular velocity (left) and acceleration (right) measurement results - s denotes the number of iterative steps in each control cycle

In Fig. 7 the measurement results are displayed for the higher derivatives of the generalized coordinates. These signals are significantly affected by the quantization error of the position measurement due to the application of the backward difference formulae in (30) and (31), that way the application of the low pass filter is necessary. The feedback noise can be further decreased by the use of higher resolution encoder.

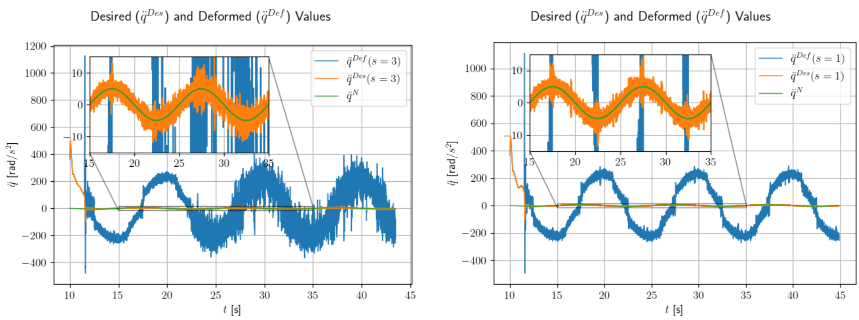

Figure 8
Deformed and desired values of the second derivative of the generalized coordinates for the multiple iterative step case (left) and the single step case (right)

Figure 8 displays the essence of the RFPT method. It is clearly visible that the deformed value $\ddot{q}^{Def}(t)$ is significantly different from the desired one $\ddot{q}^{Des}(t)$ due to the applied adaptive deformation. Furthermore, the desired trajectory is nicely implemented as $\ddot{q}^{Des}(t) \approx \ddot{q}^{N}(t)$. On the other hand, it also reveals that the proposed modification makes the controller more noise sensitive due to the repeated iterative steps.

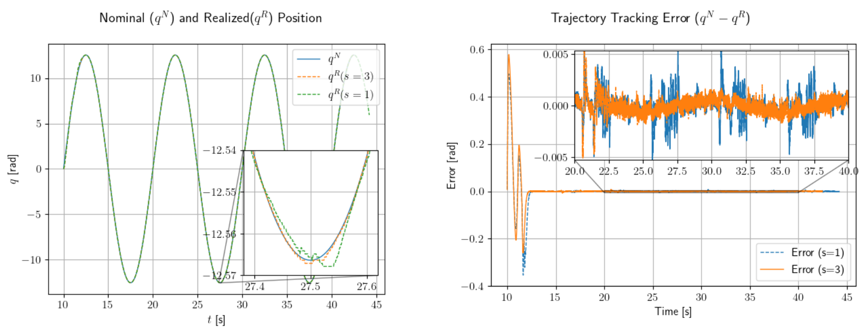

Figure 9
Angular Position of the output shaft of the DC motor (left) and trajectory tracking error (right) with the spring mounted on the motor shaft- s denotes the number of iterative steps in each control cycle

The advantage of concurrent model identification and multiple iterative steps are more evident in the second experimental scenario involving time-varying loading conditions, as illustrated by the spring attached to the motor shaft. In the case of $s = 1$ step RFPT method, that does not utilize the identified Hammerstein model, oscillations can be observed in angular position of the motors shaft in the low velocity regime as shown in the left-hand side of Fig. 9. On the other hand, precise trajectory tacking was maintained in the case of $s = 3$ iterative steps without oscillations. Further comparison can be made based on Table 1. It reveals the increased robustness of the controller, since in the case of $s = 1$ iterative steps all performance measures exhibited increasing nature under time varying load condition, however with $s = 3$ iterative steps performance measures were kept in the same range. All in all, the proposed solution seems more robust against modelling deficiencies due to the increased adaptation speed of the controller.

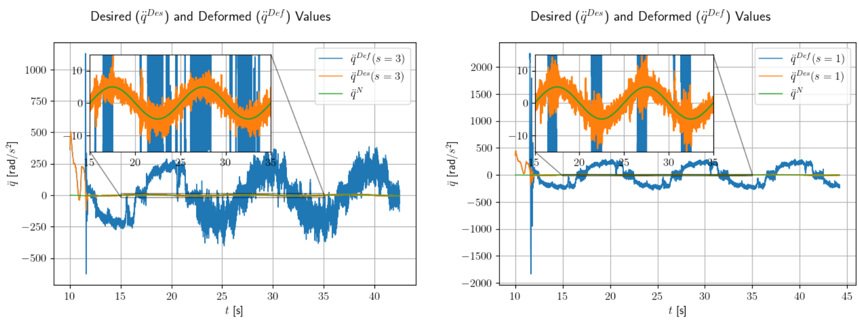

Figure 10
Deformed and desired values of the second derivative of the generalized coordinates for the multiple iterative step case (left) and the single step case (right)

5 Conclusion

In this paper a new variation of the RFPT control method was proposed where, concurrent model parameter identification of a nonlinear Hammerstein model and adaptive control was applied. The solution was inspired by the modern data driven control techniques where some kind of general model form is filled in with data, based on some fresh observation of the system response, that way building a meaningful model of the controlled system. The proposed control method involves the implementation of multiple iterative steps within each control cycle. These iterations are executed based on the forecasted system response, as determined by the identified Hammerstein model. The proposed solution can be applied for a class of nonlinear systems with second order dynamics, that are subject to actuator dead-zone or friction nonlinearities, where the conventional RFPT controller is less efficient. As an example, an important application area is cutting processes. Due to material inhomogeneity or the rough surface of the raw material, a continuously changing chip cross-section is created. Because of this, the machining process must be continuously controlled [72]. The experimental results presented in this paper, demonstrated enhanced control performance, particularly in the low-velocity regime, in the case of a DC motor control application. Furthermore, an improvement in the robustness of the controller was observed under varying loading conditions of the DC motor. On the other-hand, the noise sensitivity of the proposed solution was observed, that limits the number iterative steps in each control cycle.

Acknowledgement

We acknowledge the support of this work by the Doctoral School of Applied Informatics and Applied Mathematics of Óbuda University. This research was supported by the ÚNKP-23-3-II New National Excellence Program of the Ministry for Culture and Innovation from the source of the National Research, Development and Innovation Fund.

References

[1] R. F. Drenick and R. A. Shahbender, ”Adaptive servomechanisms,” in Transactions of the American Institute of Electrical Engineers, Part II: Applications and Industry, vol. 76, no. 5, pp. 286-292, Nov. 1957, doi: 10.1109/TAI.1957.6367242.

[2] H. Philip Whitaker, J. Yamron, and A. Kezer, Design of Model Reference Adaptive Control Systems for Aircraft. Massachusetts Institute of Technology. Instrumentation Laboratory, 1958.

[3] Iven M.Y. Mareels, Brian D.O. Anderson, R. R. Bitmead, M. Bodson, and S. S. Sastry, “Revisiting the Mit Rule for Adaptive Control,” IFAC proceedings volumes, vol. 20, no. 2, pp. 161–166, Jul. 1987, doi: 10.1016/s1474-6670(17)55954-6.

[4] Z. T. Dydek, A. M. Annaswamy and E. Lavretsky, ”Adaptive Control and the NASA X-15-3 Flight Revisited,” in IEEE Control Systems Magazine, vol. 30, no. 3, pp. 32-48, June 2010, doi: 10.1109/MCS.2010.936292.

[5] A.M. Lyapunov: A General Task about the Stability of Motion. (in Russian), Ph.D. Thesis, University of Kazan, Tatarstan (Russia), 1892.

[6] A.M. Lyapunov: Stability of Motion, Academic Press, New-York and London, 1966.

[7] P. Parks, ”Liapunov redesign of model reference adaptive control systems,” in IEEE Transactions on Automatic Control, vol. 11, no. 3, pp. 362-367, July 1966, doi: 10.1109/TAC.1966.1098361.

[8] Juan Carlos Travieso-Torres, Abdiel Ricaldi-Morales, A. Véliz-Tejo, and F. Leiva-Silva, “Robust Cascade MRAC for a Hybrid Grid-Connected Renewable Energy System,” Processes, vol. 11, no. 6, pp. 1774–1774, Jun. 2023, doi: https://doi.org/10.3390/pr11061774.

[9] X. Zhou, Z. Wang and J. Wang, ”Automated Vehicle Path Following: A Non-Quadratic-Lyapunov-Function-Based Model Reference Adaptive Control Approach With C∞-Smooth Projection Modification,” in IEEE Transactions on Intelligent Transportation Systems, vol. 23, no. 11, pp. 21653-21664, Nov. 2022, doi: 10.1109/TITS.2022.3182928.

[10] D. Zhang and B. Wei, “A review on model reference adaptive control of robotic manipulators,” Annual Reviews in Control, vol. 43, pp. 188–198, 2017, doi: https://doi.org/10.1016/j.arcontrol.2017.02.002.

[11] M. W. Spong and R. Ortega, ”On adaptive inverse dynamics control of rigid robots,” in IEEE Transactions on Automatic Control, vol. 35, no. 1, pp. 92-95, Jan. 1990, doi: 10.1109/9.45152

[12] H. Wang and Y. Xie, “Adaptive inverse dynamics control of robots with uncertain kinematics and dynamics,” Automatica, vol. 45, no. 9, pp. 2114–2119, Sep. 2009, doi: https://doi.org/10.1016/j.automatica.2009.05.011.

[13] J.-J. E. Slotine and W. Li, “Composite adaptive control of robot manipulators,” Automatica, vol. 25, no. 4, pp. 509–519, Jul. 1989, doi: 10.1016/0005-1098(89)90094-0.

[14] P. Kokotović and M. Arcak, “Constructive nonlinear control: a historical perspective,” Automatica, vol. 37, no. 5, pp. 637–662, May 2001, doi: 10.1016/s0005-1098(01)00002-4.

[15] N. Koksal, H. An, and B. Fidan, “Backstepping-based adaptive control of a quadrotor UAV with guaranteed tracking performance,” ISA Transactions, vol. 105, pp. 98–110, Oct. 2020, doi: https://doi.org/10.1016/j.isatra.2020.06.006.

[16] X. Wang and S. Wang, “Adaptive Back-stepping Control of Servo Systems With Asymmetric Dead Zone,” International Journal of Control Automation and Systems, vol. 22, no. 9, pp. 2711–2722, Sep. 2024, doi: https://doi.org/10.1007/s12555-024-0202-z.

[17] J. K. Tar, J. F. Bitó, László Nádai, and A. Tenreiro, “Robust fixed point transformations in adaptive control using local basin of attraction,” Acta Polytechnica Hungarica, vol. 6, no. 1, pp. 21–38, Dec. 2009.

[18] A. Dineva, J. K. Tar, A. Várkonyi-Kóczy and V. Piuri, ”Adaptive controller using fixed point transformation for regulating propofol administration through wavelet-based anesthetic value,” 2016 IEEE International Symposium on Medical Measurements and Applications (MeMeA), Benevento, Italy, 2016, pp. 1-6, doi: 10.1109/MeMeA.2016.7533813.

[19] B. Csanádi and J. K. Tar, ”Selection of kinematic requirements for RFPT-based adaptive anaesthesia control,” 2016 IEEE 11th International Symposium on Applied Computational Intelligence and Informatics (SACI), Timisoara, Romania, 2016, pp. 181-186, doi: 10.1109/SACI.2016.7507365.

[20] G. Eigner, P. Horváth, J. K. Tar, I. J. Rudas and L. Kovács, ”Application of Robust Fixed Point Control in Case of T1DM,” 2015 IEEE International Conference on Systems, Man, and Cybernetics, Hong Kong, China, 2015, pp. 2459-2464, doi: 10.1109/SMC.2015.430.

[21] Jelena Tašić, M. Takács, and Levente Kovács, “Control Engineering Methods for Blood Glucose Levels Regulation,” Acta Polytechnica Hungarica, vol. 19, no. 7, pp. 127–152, Jan. 2022, doi: https://doi.org/10.12700/aph.19.7.2022.7.7.

[22] B. Csanádi, J. K. Tar and J. F. Bitó, ”Fixed point transformation-based adaptive control of the Furuta Pendulum,” 2016 IEEE 17th International Symposium on Computational Intelligence and Informatics (CINTI), Budapest, Hungary, 2016, pp. 000049-000054, doi: 10.1109/CINTI.2016.7846378.

[23] B. Varga, J. K. Tar and R. Horváth, ”Fixed Point Iteration-based Adaptive Control with Output Filtering,” 2023 IEEE 21st Jubilee International Symposium on Intelligent Systems and Informatics (SISY), Pula, Croatia, 2023, pp. 000509-000514, doi: 10.1109/SISY60376.2023.10417912.

[24] I.J. Rudas, J.K. Tar, and T.A. Várkonyi. Novel adaptive synchronization of different chaotic Chua circuits. Proc. of the Special International Conference on Complex Systems: Synergy of Control, Communications and Computing (ETAI COSY 2011), Ohrid, Macedonia, Sept. 16 – 20 2011, pages 109–114, 2011.

[25] J.F. Bitó and J.K. Tar. Fixed point transformation-based adaptive control of the Hodgkin-Huxley neuron. Proc. of the Workshop on Information Technology and Bionics – Symposium in Memory of Tamás Roska, 23-24 June, 2015, Pázmány University ePress, Budapest, Hungary, pages 69–72, 2015.

[26] Y. Cheng, X. Ren, D. Zheng and L. Li, ”Non-Linear Bandwidth Extended-State-Observer Based Non-Smooth Funnel Control for Motor-Drive Servo Systems,” in IEEE Transactions on Industrial Electronics, vol. 69, no. 6, pp. 6215-6224, June 2022, doi: 10.1109/TIE.2021.3095811.

[27] B. Armstrong, O. Khatib and J. Burdick, ”The explicit dynamic model and inertial parameters of the PUMA 560 arm,” Proceedings. 1986 IEEE International Conference on Robotics and Automation, San Francisco, CA, USA, 1986, pp. 510-518, doi: 10.1109/ROBOT.1986.1087644.

[28] Z. Song, J. Yi, D. Zhao, and X. Li, “A computed torque controller for uncertain robotic manipulator systems: Fuzzy approach,” Fuzzy Sets and Systems, vol. 154, no. 2, pp. 208–226, Sep. 2005, doi: https://doi.org/10.1016/j.fss.2005.03.007.

[29] P. I. Corke and B. Armstrong-Helouvry, ”A search for consensus among model parameters reported for the PUMA 560 robot,” Proceedings of the 1994 IEEE International Conference on Robotics and Automation, San Diego, CA, USA, 1994, pp. 1608-1613 vol.2, doi: 10.1109/ROBOT.1994.351360.

[30] S. Banach, “Sur les opérations dans les ensembles abstraits et leur application aux équations intégrales,” (About the Operations in the Abstract Sets and Their Application to Integral Equations) Fundamenta Mathematicae, vol. 3, pp. 133–181, 1922, doi: https://doi.org/10.4064/fm-3-1-133-181.

[31] A. Dineva, J.K. Tar and A. Várkonyi-Kóczy: Novel Generation of Fixed Point Transformation for the Adaptive Control of a Nonlinear Neuron Model, Proc. of the 2015 IEEE International Conference on Systems, Man, and Cybernetics, pp. 987-992, doi:10.1109/SMC.2015.179.

[32] A. Dineva, J. K. Tar and A. Várkonyi-Kóczy, "Novel Generation of Fixed Point Transformation for the Adaptive Control of a Nonlinear Neuron Model," 2015 IEEE International Conference on Systems, Man, and Cybernetics, Hong Kong, China, 2015, pp. 987-992, doi: 10.1109/SMC.2015.179.

[33] B. Csandi, P. Galambos, J. K. Tar, G. Györök and A. Serester, "A Novel, Abstract Rotation-Based Fixed Point Transformation in Adaptive Control," 2018 IEEE International Conference on Systems, Man, and Cybernetics (SMC), Miyazaki, Japan, 2018, pp. 2577-2582, doi: 10.1109/SMC.2018.00441.

[34] H. Issa and J. K. Tar, "Noise Sensitivity Reduction of the Fixed Point Iteration-based Adaptive Control," 2021 IEEE 19th International Symposium on Intelligent Systems and Informatics (SISY), Subotica, Serbia, 2021, pp. 171-176, doi: 10.1109/SISY52375.2021.9582514.

[35] D.G. Luenberger. Introduction to Dynamic Systems: Theory, Models, and Applications. John Wiley & Sons, New York, 1979.

[36] J. K. Tar, J. F. Bitó and I. J. Rudas, "Replacement of Lyapunov's direct method in Model Reference Adaptive Control with Robust Fixed Point Transformations," 2010 IEEE 14th International Conference on Intelligent Engineering Systems, Las Palmas, Spain, 2010, pp. 231-235, doi: 10.1109/INES.2010.5483841.

[37] B. Varga, J. K. Tar, and Richárd Horváth, "Fractional order inspired iterative adaptive control," Robotica, vol. 42, no. 2, pp. 482–509, Dec. 2023, doi: https://doi.org/10.1017/s0263574723001595.

[38] B. Varga, Richárd Horváth, and J. K. Tar, "Fractional Order Calculus-Inspired Kinematic Design in Adaptive Control," Mechanisms and machine science, pp. 218–225, Jan. 2022, doi: 10.1007/978-3-031-04870-8_26.

[39] M. Stefanoni, D. Csík, P. Sarcevic, Á. Odry and J. K. Tar, "Adaptive Control Lyapunov Function-Based Controller Using Fixed Point Iteration," 2024 IEEE 18th International Symposium on Applied Computational Intelligence and Informatics (SACI), Timisoara, Romania, 2024, pp. 000479-000484, doi: 10.1109/SACI60582.2024.10619780.

[40] A. Dineva, A. R. Varkonyi-Kóczy and J. K. Tar, "Combination of RFPT-based adaptive control and classical model identification," 2014 IEEE 12th International Symposium on Applied Machine Intelligence and Informatics (SAMI), Herl'any, Slovakia, 2014, pp. 173-178, doi: 10.1109/SAMI.2014.6822401.

[41] J. K. Tar, I. Rudas, A. Dineva, and A. Várkonyi Kóczy, "Stabilization of a Modified Slotine-Li Adaptive Robot Controller by Robust Fixed Point Transformations," vol. 21, pp. 35–40, Jan. 2014.

[42] M. Merei and J. K. Tar, "Adaptive Backstepping Control Design for Nonlinear System," 2023 IEEE 17th International Symposium on Applied Computational Intelligence and Informatics (SACI), Timisoara, Romania, 2023, pp. 000147-000152, doi: 10.1109/SACI58269.2023.10158606.

[43] H. Issa and J. K. Tar, ”On the Limitations of PSO in Cooperation with FPI-based Adaptive Control for Nonlinear Systems,” 2022 IEEE 26th International Conference on Intelligent Engineering Systems (INES), Georgioupolis Chania, Greece, 2022, pp. 000181-000186, doi: 10.1109/INES56734.2022.9922654.

[44] H. Issa and J. K. Tar, “Improvement of an Adaptive Robot Control by Particle Swarm Optimization-Based Model Identification,” Mathematics, vol. 10, no. 19, pp. 3609–3609, Oct. 2022, doi: https://doi.org/10.3390/math10193609.

[45] B. Varga, J. K. Tar, and Richárd Horváth, “Fixed Point Iteration-Based Adaptive Control Improved with Parameter Identification,” Mechanisms and machine science, pp. 383–390, Jan. 2023, doi: 10.1007/978-3-031-32606-6_45

[46] B. Varga, R. Horváth and J. K. Tar, ”Adaptive Control of a Nonlinear System Avoiding State Estimation,” 2022 IEEE 20th Jubilee World Symposium on Applied Machine Intelligence and Informatics (SAMI), Poprad, Slovakia, 2022, pp. 000323-000328, doi: 10.1109/SAMI54271.2022.9780781.

[47] K. Kósi and A. Awudu, ”Increasing The Convergence Speed of Robust Fixed Point Transformaton-based Adaptive Control by Steffensen's Method in SISO Case,” 2022 IEEE 20th Jubilee International Symposium on Intelligent Systems and Informatics (SISY), Subotica, Serbia, 2022, pp. 285-290, doi: 10.1109/SISY56759.2022.10036260.

[48] A. Atinga, K. Kósi and J. K. Tar, ”Improving the Tracking Precision of a Robust Sliding Mode Controller Using Steffensen's Convergence Accelerator Strategy,” 2024 IEEE 18th International Symposium on Applied Computational Intelligence and Informatics (SACI), Timisoara, Romania, 2024, pp. 000285-000290, doi: 10.1109/SACI60582.2024.10619830.

[49] Awudu Atinga, Krisztián Kósi, and J. K. Tar, “Multivariable Steffensen's Accelerator in Adaptive Sliding Mode Control,” Acta Polytechnica Hungarica, vol. 21, no. 10, pp. 413–438, Jan. 2024, doi: https://doi.org/10.12700/aph.21.10.2024.10.26.

[50] I. Lovas, “Fixed Point, Iteration-based, Adaptive Controller Tuning, Using a Genetic Algorithm,” Acta Polytechnica Hungarica, vol. 19, no. 2, pp. 59–77, Jan. 2022, doi: https://doi.org/10.12700/aph.19.2.2022.2.4.

[51] S. Wang and J. Na, ”Parameter Estimation and Adaptive Control for Servo Mechanisms With Friction Compensation,” in IEEE Transactions on Industrial Informatics, vol. 16, no. 11, pp. 6816-6825, Nov. 2020, doi: 10.1109/TII.2020.2971056.

[52] Z. Zhao, Z. Tan, Z. Liu, M. O. Efe and C. K. Ahn, ”Adaptive Inverse Compensation Fault-Tolerant Control for a Flexible Manipulator With Unknown Dead-Zone and Actuator Faults,” in IEEE Transactions on Industrial Electronics, vol. 70, no. 12, pp. 12698-12707, Dec. 2023, doi: 10.1109/TIE.2023.3239926.

[53] M. Nordin and P.-O. Gutman, “Controlling mechanical systems with backlash—a survey,” Automatica, vol. 38, no. 10, pp. 1633–1649, Oct. 2002, doi: 10.1016/S0005-1098(02)00047-X.

[54] R. Zhang, Z. Wang, N. Bailey, and P. Keogh, “Experimental assessment and feedforward control of backlash and stiction in industrial serial robots for low-speed operations,” International Journal of Computer Integrated Manufacturing, vol. 36, no. 3, pp. 393–410, Jul. 2022, doi: https://doi.org/10.1080/0951192x.2022.2090609.

[55] L. Freidovich, A. Robertsson, A. Shiriaev and R. Johansson, ”LuGre-Model-Based Friction Compensation,” in IEEE Transactions on Control Systems Technology, vol. 18, no. 1, pp. 194-200, Jan. 2010, doi: 10.1109/TCST.2008.2010501.

[56] K. Narendra and P. Gallman, ”An iterative method for the identification of nonlinear systems using a Hammerstein model,” in IEEE Transactions on Automatic Control, vol. 11, no. 3, pp. 546-550, July 1966, doi: 10.1109/TAC.1966.1098387.

[57] T. Kara and İ. Eker, “Nonlinear modeling and identification of a DC motor for bidirectional operation with real time experiments,” Energy Conversion and Management, vol. 45, no. 7–8, pp. 1087–1106, May 2004, doi: https://doi.org/10.1016/j.enconman.2003.08.005.

[58] K. P. Fruzzetti, A. Palazoğlu, and K. A. McDonald, “Nolinear model predictive control using Hammerstein models,” Journal of Process Control, vol. 7, no. 1, pp. 31–41, Feb. 1997, doi: 10.1016/s0959-1524(97)80001-b.

[59] J. Hou, H. Su, C. Yu, F. Chen and P. Li, ”Bias-Correction Errors-in-Variables Hammerstein Model Identification,” in IEEE Transactions on Industrial Electronics, vol. 70, no. 7, pp. 7268-7279, July 2023, doi: 10.1109/TIE.2022.3199931.

[60] Nezmin Kayedpour, A. E. Samani, M. De, L. Vandevelde, and Guillaume Crevecoeur, “Model Predictive Control With a Cascaded Hammerstein Neural Network of a Wind Turbine Providing Frequency Containment Reserve,” IEEE Transactions on Energy Conversion, vol. 37, no. 1, pp. 198–209, Mar. 2022, doi: https://doi.org/10.1109/tec.2021.3093010.

[61] Lennart, L. (1999). System identification: theory for the user. PTR Prentice Hall, Upper Saddle River, NJ, 28, 540.

[62] T. J. Harris, J. Astrom, and B. Wittenmark, “Adaptive Control,” Technometrics, vol. 33, no. 4, pp. 487–487, Nov. 1991, doi: https://doi.org/10.2307/1269433.

[63] E. C. Ifeachor and B. W. Jervis, Digital signal processing: a practical approach. Pearson Education, 2002.

[64] R.-C. Roman, R.-E. Precup, E. M. Petriu, and F. Dragan, “Combination of Data-Driven Active Disturbance Rejection and Takagi-Sugeno Fuzzy Control

with Experimental Validation on Tower Crane Systems," Energies, vol. 12, no. 8, p. 1548, Apr. 2019, doi: https://doi.org/10.3390/en12081548.

[65] Radu-Emil Precup, Mircea-Bogdan Radac, R.-C. Roman, and E. M. Petriu, "Model-free sliding mode control of nonlinear systems: Algorithms and experiments," Information Sciences, vol. 381, pp. 176–192, Mar. 2017, doi: https://doi.org/10.1016/j.ins.2016.11.026.

[66] M. C. Campi, A. Lecchini, and S. M. Savaresi, "Virtual reference feedback tuning: a direct method for the design of feedback controllers," Automatica, vol. 38, no. 8, pp. 1337–1346, Aug. 2002, doi: 10.1016/s0005-1098(02)00032-8.

[67] Z. Hou and S. Jin, "A Novel Data-Driven Control Approach for a Class of Discrete-Time Nonlinear Systems," in IEEE Transactions on Control Systems Technology, vol. 19, no. 6, pp. 1549-1558, Nov. 2011, doi: 10.1109/TCST.2010.2093136

[68] Roman, R. C., Radac, M. B., Precup, R. E., Petriu, E. M. (2016). Data-driven model-free adaptive control tuned by virtual reference feedback tuning. Acta Polytechnica Hungarica, 13(1), 83-96.

[69] A. Atinga and J. K. Tar, "Application of Abstract Rotations in Data Driven Modeling Supported by Fixed Point Iteration-based Adaptive Control*," 2023 European Control Conference (ECC), Bucharest, Romania, 2023, pp. 1-6, doi: 10.23919/ECC57647.2023.10178172.

[70] D. Fényes, B. Németh, P. Gáspár, D. Pup and F. Szauter, "Study on a road surface estimation method based on big data analysis," 2019 IEEE 13th International Symposium on Applied Computational Intelligence and Informatics (SACI), Timisoara, Romania, 2019, pp. 57-62, doi: 10.1109/SACI46893.2019.9111487.

[71] D. Fényes, B. Németh, and P. Gáspár, "Design of LPV control for autonomous vehicles using the contributions of big data analysis," International Journal of Control, pp. 1–12, Jan. 2021, doi: https://doi.org/10.1080/00207179.2021.1876922.

[72] Richárd Horváth, Livija Cveticanin, and Ivona Ninkov, "Prediction of Surface Roughness in Turning Applying the Model of Nonlinear Oscillator with Complex Deflection," Mathematics, vol. 10, no. 17, pp. 3214–3214, Sep. 2022, doi: https://doi.org/10.3390/math10173214.